Electrochemical determination of microRNAs based on isothermal strand-displacement polymerase reaction coupled with multienzyme functionalized magnetic micro-carriers.

Ma, W; Situ, B; Lv, W; Li, B; Yin, X; Vadgama, P; Zheng, L; Wang, W

For additional information about this publication click this link.
http://qmro.qmul.ac.uk/xmlui/handle/123456789/12049
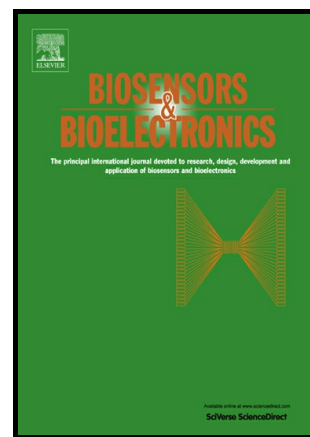
Author's Accepted Manuscript

Electrochemical determination of microRNAs based on isothermal strand-displacement polymerase reaction coupled with multienzyme functionalized magnetic micro-carriers

Wen Ma, Bo Situ, Weifeng Lv, Bo Li, Xiaomao Yin, Pankaj Vadgama, Wen Wang, Lei Zheng

Cite this article as: Wen Ma, Bo Situ, Weifeng Lv, Bo Li, Xiaomao Yin, Pankaj Vadgama, Wen Wang and Lei Zheng, Electrochemical determination of microRNAs based on isothermal strand-displacement polymerase reaction coupled with multienzyme functionalized magnetic micro-carriers, *Biosensor and Bioelectronic,* http://dx.doi.org/10.1016/j.bios.2015.12.064

Electrochemical determination of microRNAs based on isothermal strand-displacement polymerase reaction coupled with multienzyme functionalized magnetic micro-carriers

Wen Ma [a,b,1], Bo Situ [a,b,1], Weifeng Lv [a,b], Bo Li [a,b], Xiaomao Yin [c], Pankaj Vadgama [d], Wen Wang [d,*], Lei Zheng [a,b,*]

[a] *Department of Laboratory Medicine, Nanfang Hospital, Southern Medical University, Guangzhou 510515, PR China*

[b] *Guangdong Engineering and Technology Research Center for Rapid Diagnostic Biosensor, Southern Medical University, Guangzhou, Guangdong Province 510900, PR China*

[c] *Department of Laboratory Medicine, The Fifth Affiliated Hospital of Southern Medical University, Guangzhou, Guangdong Province 510900, PR China*

[d] *School of Engineering and Materials Science, Queen Mary, University of London, London E1 4NS, UK*

* Corresponding authors. Tel.: +86 20 61642147; fax: +86 20 62787681.

E-mail addresses: nfyyzhenglei@smu.edu.cn (L. Zheng),

wen.wang@qmul.ac.uk(W. Wang)

[1] W. M. and B. S. contributed equally to this study.

Abstract

MicroRNAs (miRNAs) show great potential for disease diagnostics due to their specific molecular profiles. Detection of miRNAs remains challenging and often requires sophisticated platforms. Here we report a multienzyme-functionalized magnetic microcarriers-assisted isothermal strand-displacement polymerase reaction (ISDPR) for quantitative detection of miRNAs. Magnetic micro-carriers (MMCs) were functionalized with molecular beacons to enable miRNAs recognition and magnetic separation. The target miRNAs triggered a phi29-mediated ISDPR, which can produce biotin-modified sequences on the MMCs. Streptavidin-alkaline phosphatase was then conjugated to the MMC surface through biotin-streptavidin interactions. In the presence of 2-phospho-L-ascorbic acid, miRNAs were quantitatively determined on a screen-printed carbon electrode from the anodic current of the enzymatic product. We show that this method enables detection of miRNAs as low as 9 fM and allows the discrimination of one base mismatched sequence. The proposed method was also successfully applied to analyze miRNAs in clinical tumor samples. This paper reports a new strategy for miRNAs analysis with high sensitivity, simplicity, and low cost. It would be particularly useful for rapid point-of-care testing of miRNAs in clinical laboratory.

1. Introduction

MicroRNAs (miRNAs) are a novel class of small non-coding RNA molecules (19 – 24 nucleotides in length) that play vital roles in regulating gene expression(Ameres and Zamore 2013; Valoczi et al. 2004). In the past decade, considerable studies have revealed that miRNAs are associated with diverse pathological processes such as cancers, rheumatic diseases, myocardial injury, and neurological disorders(Ameres and Zamore 2013; Lewis 2014; Lin and Gregory 2015; Pers and Jorgensen 2013; Wang et al. 2015)(Lewis 2014; Lin and Gregory 2015; Pers and Jorgensen 2013; Wang et al. 2015). Recent discoveries have also confirmed the existence of miRNAs in serum and other body fluids such as urine, saliva(Bahn et al. 2015; Lagatie et al. 2014; Wang et al. 2015). Since the levels of disease-specific miRNAs in biological samples are stable and reproducible, miRNAs are believed to hold great potential as a new class of next-generation biomarkers.

For the optimized detection of miRNA especially in clinical samples, it is desirable to combine high sensitivity and selectivity together with assay simplicity. Electrochemical detection, as an alternative to optical methods is promising to meet the requirements due to its wide detection range, short time consumption, controlled reaction system, easy miniaturization read, high sensitivity and signal to-noise ratio. Currently, efforts have been made to develop sensitive electrochemical sensors for the detection of low- abundance miRNAs(Campuzano et al. 2014; Hamidi-Asl et al. 2013).

Nuclease based signal amplification strategies have been established which

involve rolling circle amplification (RCA)(Yao et al. 2014; Zhu et al. 2015), hybridization chain reaction(HCR), loop-mediated amplification(Liu et al. 2015; Zhang et al. 2014), exonuclease assisted signal amplification(Huang et al. 2014; Wang et al. 2014) and target miRNA recycling amplification(Li et al. 2015; Shi et al. 2015). The recently reported isothermal strand-displacement polymerase reaction (ISDPR)(Dong et al. 2012) has been shown as an effective method in target recycling amplification which has been widely used in fluorescent assays for the detection of nucleic acid. However, to date, ISDPR has rarely been applied in electrochemical assays.

ISDPR is based on lengthening of a new strand to replace the target sequences which are released to initiate a new polymerization reaction. However, bst DNA polymerase commonly used in ISDPR requires a high temperature of 60−72 ℃ for optimum enzymatic activity(Shi et al. 2014; Zou et al. 2014). As a result, the amplification products with bst DNA polymerase might contain a large amount of byproducts of the nontarget DNA fragments likely decrease the efficiency of the amplification(Chen et al. 2015). To address this problem, it was reported that phi29 DNA polymerase has the abilities of extreme strand displacement and high fidelity continuous polymerization at temperatures between 30 and 40 ℃(Alsmadi et al. 2009). Therefore, it was chosen the phi29 DNA polymerase with more accurate and comprehensive products to improve efficiency of the ISDPR for signal amplification. Herein, we report an electrochemical biosensor for the amplified detection of miRNA that combines the advantages of both target enrichment by ISDPR and signal

amplification by an enzyme catalyzed reaction (Fig.1). Functionalized magnetic micro-carriers (MMCs) were utilized as hosts for enzyme loading, which can serve as versatile carriers and have been used for separation, catalysis and targeted delivery(Radwan and Azzazy 2009). In combination with MMCs, ISDPR can continue the cycle-after-cycle process of hybridization, polymerization and displacement to constantly produce new DNA sequences, and thereby increase sensitivity. Furthermore, the enzymatic reaction was found effectively compensate sensitivity loss through fluorescence quenching and high background and the large instrument requirement of isothermal amplification with optical detection, and successfully generate the output electrochemical signals offered the potential for signal amplification, further improving the sensitivity. In principle, such an ISDPR-based biosensor could detect miRNAs at 9 fM with a linear relationship between 10 and 10 nM. With the inherent advantages of ISDPR and electrochemical sensing technology, a biosensor that can be used to perform both processes could be extensively applied to detect miRNA.

2. Experimental

2.1. Chemicals and reagents

High-performance liquid chromatography-purified oligonucleotides were synthesized by Takara Biotechnology Company Ltd. (Dalian, China). The sequences are illustrated in Table S1. DNA marker, deoxyribonucleoside triphosphates (dNTPs), deoxyadenosine triphosphate (dATP), deoxythymidine triphosphate (dTTP),

deoxyguanosine triphosphate (dGTP), RNase inhibitor, and DEPC-treated water were also purchased from TaKaRa Bio Inc. (Dalian, China). Functional MMCs (1.02 μm, 10 mg/mL) were obtained from Invitrogen (Norway). MiVanaTM miRNA Isolation kit was purchased from Life Technologies (USA). All-in-One[TM] miRNA qRT-PCR Detection System Handbook for the quantitative detection of mature miRNA was purchased from GeneCopoeia (USA). Phi29 DNA polymerase was obtained from New England Biolabs Inc. (USA). Biotinylated deoxycytidine triphosphate (dCTP) was purchased from PromoKine (Germany) and agarose was obtained from Biowest (Spain). Streptavidin–alkaline phosphatase (Sa–ALP), 1-ethyl-3-(3-dimethylaminopropyl) carbodiimide (EDC), and N-hydroxysuccinimide (NHS) were purchased from Sigma-Aldrich (USA).

2.2. Apparatus

Electrochemical experiments were carried out in a CH660C electrochemical workstation (Shanghai CH Instrument, China). Disposable screen-printed carbon electrodes (SPCEs) were obtained from DropSens (Spain). The SPCE exhibits a conventional three-electrode configuration: a carbon working electrode (4 mm diameter), a carbon counter electrode, and a silver reference electrode. A sensor connector (DropSens, Spain) connects the SPCE to the electrochemical workstation. Agarose gel electrophoresis results were photographed and visualized through UV transillumination by using a Gel DocTM 2000 system (Bio-Rad, USA). Fluorescence results were obtained through confocal laser scanning microscopy performed in a FV10i-W system (Olympus, Japan) and microplate reader by using an AutoPMT

optimization system of SpectraMax M5 (Molecular Devices, USA). Real-time quantitative PCR was performed in a ABI 7500 Fast Real-time PCR system (Applied Biosystems, USA).

2.3 Modification of MMCs

The conjugates between MMCs and DNA sequences were prepared using the following method. In brief, 0.5 ml of 10 mg/ml MMC suspension was washed thrice with 1 ml of 100 mM MES buffer at pH 4.8 and then resuspended in 100 μl of the same buffer. In a separate tube, the suspension was mixed with 5′ amine modified oligonucleotide (10 nmol) and 40 μl of 1.25 M EDC in 100 mM MES to a total volume of 100 μl. Afterward, the oligo/EDC solution was added to the MMCs, mixed by vortexing for 10 s, and incubated at room temperature under constant stirring overnight. The modified MMCs were washed thrice with 0.25 M Tris–HCl buffer [0.01% (w/v) Tween-20, pH = 8.0] for 30 min to quench the unreacted activated carboxylic acid groups. The modified MMCs were then dispersed in 1 mL of 20 mM Tris–HCl buffer [1 mM EDTA, 0.5% (w/v) BSA, pH = 8.0] and stored at 4 ℃ for later use.

2.4 Isothermal strand-displacement polymerization reaction (ISDPR)

The polymerase-based ISDPR was performed by mixing 5 μl of molecular beacon (MB)-modified MMCs (5 mg/ml), 5 μl of primer (10 μM), 2 μl of phi29 DNA polymerase, 1 μl of dNTPs (1 mM dATP, 1 mM dTTP, 1 mM dGTP, 1 mM bio-dCTP), and varying concentrations of the target miRNA to a final volume of 50 μl in a buffer containing 20 mM Tris-HCl, 10 mM $(NH_4)_2SO_4$, 15 mM KCl, 2 mM $MgSO_4$, 0.1%

Tween-20 (pH 7.4); the resulting mixture was subsequently incubated at 37 ℃ for 120

min with gentle shaking. The MMCs were washed thrice with 500 μl of Tris–HCl (20

mM, pH 7.4) to remove the excess sequences.

2.5 Electrochemical detection

Then, 50 μl of Sa-ALP that was diluted 500 times was added to ISDPR product

for 15min to incubate at room temperature to form the biotin–streptavidin linkages.

Redundant enzymes were moved away by washing the MMCs twice in a magnetic

field with 500 μl Tris–HCl (20 mM, pH 7.4). And then,the MMCs were re-suspended

in 50 μl of 75 mM AAP (0.1 M Tris–HCl, pH 9.0, 1 mM $MgCl_2$) solution and

incubated for 15 min at 37 ℃ with gently shaking. The enzymatic cross-linking was

ended by adding the 2 μl of 0.1 M disodium EDTA. 5 μl of the supernatant was

mingled with 45 μl of sodium acetate buffer (0.1 M, pH 5.5) after magnetic separation.

Then, hybridization reaction mixture (50 μl) was dropped onto the SPCE reservoir

area to cover the working, counter, and reference electrodes. The electrochemical

behavior of the reaction products was examined by cyclic voltammetry (CV) and

differential pulse voltammetry (DPV). Measurements were always made in triplicate.

DPV were conducted with a potential scan range from -0.1 to 0.7 V (versus silver /

silver chloride), modulation amplitude of 0.05 V, pulse width 1 of 0.2 s, pulse width 2

of 0.05 s and sample width of 0.0167 s, in an buffer solution, which was degassed

with nitrogen for 15 min. The DPV peak current was registered as the sensor signal.

CV measurements were carried out at a scan rate of 0.1 V/s between -0.5 V and 0.65 V,

with a scan increment of 0.1V/s in the nitrogen degassed (5 min) hybridization buffer.

2.6. Clinical sample detection

We obtained the 5 breast carcinoma tissues and the same para-cancerous tissues from Breast Oncology Center of Nanfang Hospital, Southern Medical University. All breast tumors were confirmed by surgery and pathology. Total RNA was extracted by recommended miVanaTM miRNA Isolation kit and dissolved in RNase-free water. The concentration of the extracted RNA was measured by spectrophotometer using NanoDrop ND-2000. 1μg of this sample was used as template in the following detection by the proposed method and real time fluorescent quantitative PCR.

3. Results and discussion

3.1 Experimental principle of the sensing assay

The principle of this isothermal amplified detection miRNA method is shown in detail in Fig.1. A new method was developed to incorporate amino groups and multiple biotin labels within an ISDPR reaction to amplified target sequences. As shown in step A, The miRNA ISDPR detection system mainly composed of a MB-modified MMC, phi-29 DNA polymerase and a short primer. The molecular beacon (MB) acted as a template of polymerization reaction, while the target miRNA as a trigger of polymerization reaction. The miRNA detection system was activated by the conformational change of the MB, which was induced by the hybridization between the MB and the target miRNA. Subsequently, the primer annealed with the exposed 3'terminus of the opened probe and triggered a polymerase replication in the presence of dNTPs (dATP, dTTP, dGTP, bio-dCTP) and phi29 DNA polymerase. The target miRNA was simultaneously displaced by the phi29 DNA polymerase with

strand-displacement activity occurring during primer extension. Complementary DNA (cDNA) was then synthesized, forming a probe-cDNA complex. The hybridisation product was labeled with biotin by adding biotinylated dCTP to the reaction. Therefore, the process of hybridization, polymerization reaction and displacement recur in cycles , continuously producing DNA sequences. Finally, to renew the cycle, the displaced target hybridized with another probe, which triggered yet another polymerization reaction, resulting in the multiplication of the biotin-modified DNA on the surface of MMCs. In step B, Sa–ALPs were linked to the MMC surface through biotin–streptavidin conjugation after these substances were incubated with composite nanoparticles. The amount of ALP loaded on to the MMCs was related to the original amount of miRNA. MiRNA can be detected by measuring the oxidation current of ascorbic acid (AA) on a SPCE because ascorbic acid is a product of enzymatic hydrolysis. The target can be detected with high sensitivity by monitoring the increase in current intensities.

Fig. 1

3.2 Characterization of ISDPR

A model system in a solution was created by hybridizing the 5'-FAM, 3'-Dabcyl labeled MB probe and miR-21 produced during the recycling reaction to verify isothermal strand-displacement polymerase reaction (Fig.S1). The reaction progress was monitored via the emission spectrum (Fig.2). The fluorescence intensity increased as a function of increasing miR-21 concentration from 1 nM to 1 μM

(Fig.2A). Thus the miRNA target may hybridize with the immobilized MB to initiate the cycle of MB and activate the amplification process. Furthermore, the signal amplification was found to be clearly dependent on the phi29 DNA polymerase since the fluorescence signal substantially increased upon addition of it (Fig.2B), further confirming the circular strand-displacement reaction was initiated by the presence of phi29 DNA polymerase.

Fig.2

3.3 Mixing of biotin–dCTP in the sensing assay

In our approach, whether the incorporation of biotin–dCTP affects ISDPR should be determined. As shown in Fig.S2, amplicons were successfully labeled with biotin molecules by adding biotin-modified dCTP to ISDPR. The total concentration of biotinylated and natural dCTP was maintained at 1 mM, which was then used to evaluate the incorporation of biotin–dCTP in the reaction.The biotin–dCTP was mixed between 0 % and 100 %, and the products were subjected to electrophoresis in 3% agarose gel. When the system contained 100% biotinylated dCTP, the mobility of the products correspondingly decreased possibly because of the large bulk introduced by the biotin molecules(Situ et al. 2013). The evident decrease in the product shows that phi29 DNA polymerase incorporated natural dCTP with a greater efficiency than biotinylated dCTP. Therefore, 100% biotin–dCTP was chosen in the follow-up experiments to provide a high labeling rate, although the amplification yield was reduced. Compared with routine labeling approaches, such as with biotin-modified

primers(Luo et al. 2014), a major benefit of the proposed method was the uniform distribution of modifications across each DNA duplex. Thus, each product was capable of binding a large amount of enzyme by the streptavidin–biotin interaction, resulting in a multienzyme-labeling assay facilitating the signal amplification strategy(Situ et al. 2013).

3.4 Characterization of the composite nanoparticles

Magnetic nanomaterials have been extensively investigated because of their intrinsic properties and potential new applications. Carboxyl-modified MMCs possess the required magnetic properties for an efficient separation from reaction mixtures by using external magnets; these MMCs also enable the ready conjugation of biomolecules through the ammonia carboxy complexation reaction(Manriquez et al. 2009). In this work, the carboxyl-modified MMCs were utilized a vehicle to load alkaline phosphatase-active conjugates of multi-enzyme-functionalized sequences.

The morphological characteristics of the composite nanoparticles were determined using a confocal microscope to verify that the probes were successfully attached to the MMC surface. The images of the MMCs and MMCs connected to the FAM-probe are shown in Fig.3A, 3B, 3C, and 3D. These findings clearly showed that fluorescence significantly increased after the FAM-probe was modified. These results indicated that the probe was successfully conjugated to the MMC surface.

Cyclic voltammetry was used to investigate the interface features on conductive surfaces. The transduction principle of the modification steps or recognition event is based on the electron-transfer in the presence of a pair of quasi-reversible redox peaks

of [Fe(CN)6]4-/3-, measured by cyclic voltammetry (CV) (Radi et al. 2005). When the nanoparticle was covered by more and more substance, it could lead to the reduced electron transfer kinetics on the surface of the electrode. In Fig.3E, a comparison between bare MMCs (curve a) and MMCs modified with MB showed a decreased signal (curve b), suggesting that the binding DNA created a barrier to interfacial electron transfer. Furthermore, significantly decreased peak currents were observed after ISDPR on the MMCs (curve c), and ISDPR on the MMCs/SA-ALP (curve d) which can be linked to further reduced electron transfer kinetics at bio-DNA-coated and protein-coated nanoparticles. These results are consistent with confocal microscopy images, confirming the conjugation of oligonucleotide and protein on the MMCs.
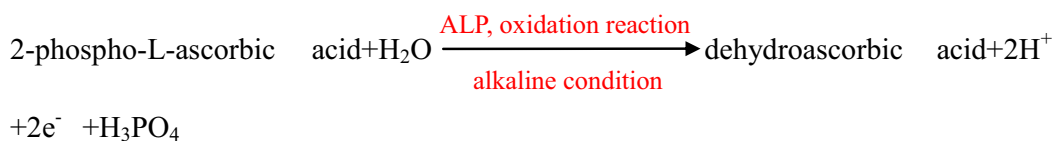
<div style="border:1px solid black; text-align:center;">

Fig.3

</div>

3.5 Electroanalysis of products and substrates of ALP

Alkaline phosphatase (ALP) catalyzes the hydrolysis of phosphate esters in an alkaline environment, resulting in the formation of an organic radical and inorganic phosphat(Wilson and Rauh 2004). In the proposed electrochemical sensing assays, the immobilized ALP catalyzes its substrate (2-phospho-L-ascorbic acid, AAP) to produce ascorbic acid (AA) as electron donor, which can provide one electron to be captured by the detector, resulting in an increased redox signal, as shown in the chemical reaction(Preechaworapun et al. 2008). The amount of ALP loaded on to the MMCs was related to the original amount of miRNA which can be detected by measuring the oxidation current of ascorbic acid (AA) on a SPCE because ascorbic

acid is a product of enzymatic hydrolysis.

Chemical reaction:

2-phospho-L-ascorbic acid+H_2O $\xrightarrow[\text{alkaline condition}]{\text{ALP, oxidation reaction}}$ dehydroascorbic acid+$2H^+$ +$2e^-$ +H_3PO_4

3.6 Optimization of assay conditions

The key experimental variables affecting the performance of the magnetic sensor were optimized on the basis of the curve inflection points of the current response of 10 nM synthetic miR-21 as the selection criterion. Different variables were tested, and the assay ranges checked for each of them. The variables selected for further analysis are summarized in Table 1, and the detailed results are shown in Fig.S3.

Table 1

3.7 The sensitivity and selectivity of the RNA biosensor

As MiRNAs represent only a small fraction of the total mass of RNA in a sample, the miRNAs amounts in real samples can be of as low as a few molecules and so a highly sensitive assay is urgently demanding. In addition, the expression level of the miRNAs varies in a dynamic range in different samples, therefore a assay which enables to measure miRNAs within a wide range of concentrations is required(Dong et al. 2013). Under optimized reaction conditions, DPV signals resulting from the reactions of different target miRNA concentrations were recorded. The sensitivity of the biosensor for the detection of target miRNA was investigated by varying the target miRNA concentration (Fig.4A). The absolute value of average current shows a good

linear correlation with the logarithm of target miRNA concentrations in the range of 10fM—10nM (Fig.4B). The linear regression equation is $I = (10^{-6}$ A$)=2.488\lg(C_{target})-1.721$, with a linear relationship coefficient r=0.989. The detection limit (3σ/S, where σ is the standard deviation of the blank solution) was calculated to be 9fM for complementary target miRNA. ISDPR sensing assay for miRNA herein has lower detection limit comparing to other recently developed electrochemical miRNA sensing assays. The proposed method shows the combined advantages by using nanoparticles coupled with enzyme-based double signal amplification (Table S2). The use of micro magnetic particles as a carrier to build up the bulk sample phase of the microRNA electrochemical detection technology avoids the need for delicate electrode preparation. Also, miRNAs can be amplified by ISDPR using molecular beacons with high specificity. The incorporation of enzyme (alkaline phosphatase) to generate the electrochemical signal offers the potential for signal amplification, further improving the sensitivity.

The small size and the sequence similarity of miRNAs in the RNA family significantly complicate miRNA detection hybridization reactions. In particular, a sequence mismatch can easily produce a false positive signal. As such, efficient strategies should be developed to enhance the specificity of miRNA profiling measurements. Thus, the specificity of the proposed RNA biosensor was investigated by detecting various RNA sequences, including target miRNA (miR-21), single-base-mismatched miR-21 (SM miR21), and three-base-mismatched miR-21 (TM miR-21), as negative controls and a sample without target as a blank control.

Fig.4C shows that the intensity of the response to miR-21 was higher than that of TM miR-21 and random RNA, although only a single base mismatch was observed. Therefore, the proposed miRNA assay exhibited good selectivity.

Fig. 4

3.8 Detection in RNA from tissue sample

To expand the applicability of the proposed approach in miRNA detection, we also investigated whether the methodology can be applied to detect target miR-21 in the RNA extracted from human breast cancer tissues and paired adjacent tissues . As shown in Table S2, the A260/280 absorbance ratios of isolated RNA were around 2.0, indicating that the RNA fraction is pure with barely analytical interference such as proteins and phenolics. Additionally, all the A260/230 values are higher than 1.6, suggesting negligible contaminants of carbohydrates and salts is detected(Ghawana et al. 2011; le Provost et al. 2007). These data show that the extracted RNA is pure with little analytical interference to the assay. The electrochemical signal intensities from the breast cancer tissues were clearly higher than those from the adjacent control tissues except a pair of specimens. The level of miR-21 detected in sample 1 was low possibly because this patient was treated with chemotherapy before surgery. In addition, our results were consistent with the reverse transcription PCR (RT-PCR) results, indeed, our method is accurate. The results also indicated that the method can distinguish the miR-21 expression between breast cancer tissues and the adjacent normal tissues; indeed, the proposed method can be recommended for clinical applications.

Fig. 5

4. Conclusions

We have developed a highly sensitive and selective miRNA detection platform based on functionalized multienzyme magnetic microcarrier assisted isothermal strand-displacement polymerase reaction to enable efficient, isothermal detection of miRNAs. Under optimized conditions, the peak currents showed a good linear relationship with the logarithm of target oligonucleotide concentrations, with a detection limit of 9 fM owning to the dual amplification of the assay. By switching the MBs, the proposed method could be extended for high throughput detection of miRNA. Therehfore, the method presented here provides a general platform to detect various target miRNAs at low levels, potentially for clinical applications. In this method, reverse transcription or large apparatus is not necessary, and a shorter assay time is required; thus, the proposed method could be applied to primary hospitals or point-of-care testing. The development of electrochemical detection also provided theoretical and practical implications for solid-state miRNA chip designs. Our results on the clinical specimens were consistent with reverse transcription PCR findings, thus, the method is reliable and is a potential candidate for a sensitive, rapid, economical, and convenient miRNA diagnostic platform.

Acknowledgements

Appendix A Supplementary data

Supplementary data associated with this article can be found in the online version.

References:

Alsmadi, O., Alkayal, F., Monies, D., Meyer, B.F., 2009. Specific and complete human genome amplification with improved yield achieved by phi29 DNA polymerase and a novel primer at elevated temperature. BMC Res Notes 2, 48.

Ameres, S.L., Zamore, P.D., 2013. Diversifying microRNA sequence and function. Nat Rev Mol Cell Biol 14(8), 475-488.

Bahn, J.H., Zhang, Q., Li, F., Chan, T.M., Lin, X., Kim, Y., Wong, D.T., Xiao, X., 2015. The landscape of microRNA, Piwi-interacting RNA, and circular RNA in human saliva. CLIN CHEM 61(1), 221-230.

Campuzano, S., Pedrero, M., Pingarron, J.M., 2014. Electrochemical genosensors for the detection of cancer-related miRNAs. ANAL BIOANAL CHEM 406(1), 27-33.

Chen, A., Gui, G.F., Zhuo, Y., Chai, Y.Q., Xiang, Y., Yuan, R., 2015. Signal-off Electrochemiluminescence Biosensor Based on Phi29 DNA Polymerase Mediated Strand Displacement Amplification for MicroRNA Detection. ANAL CHEM 87(12), 6328-6334.

Dong, H., Lei, J., Ding, L., Wen, Y., Ju, H., Zhang, X., 2013. MicroRNA: function, detection, and bioanalysis. CHEM REV 113(8), 6207-6233.

Dong, H., Zhang, J., Ju, H., Lu, H., Wang, S., Jin, S., Hao, K., Du H, Zhang, X., 2012. Highly sensitive multiple microRNA detection based on fluorescence quenching of graphene oxide and isothermal strand-displacement polymerase reaction. ANAL CHEM 84(10), 4587-4593.

Ghawana, S., Paul, A., Kumar, H., Kumar, A., Singh, H., Bhardwaj, P.K., Rani, A., Singh, R.S., Raizada, J., Singh, K., Kumar, S., 2011. An RNA isolation system for plant tissues rich in secondary metabolites. BMC Res Notes 4, 85.

Hamidi-Asl, E., Palchetti, I., Hasheminejad, E., Mascini, M., 2013. A review on the electrochemical biosensors for determination of microRNAs. TALANTA 115, 74-83.

Huang, R.C., Chiu, W.J., Li, Y.J., Huang, C.C., 2014. Detection of microRNA in tumor cells using exonuclease III and graphene oxide-regulated signal amplification. ACS Appl Mater Interfaces 6(24), 21780-21787.

Lagatie, O., Van Loy, T., Tritsmans, L., Stuyver, L.J., 2014. Viral miRNAs in plasma and urine divulge JC polyomavirus infection. VIROL J 11, 158.

le Provost, G., Herrera, R., Paiva, J.A., Chaumeil, P., Salin, F., Plomion, C., 2007. A micromethod for high throughput RNA extraction in forest trees. BIOL RES 40(3), 291-297.

Lewis, S., 2014. Neurological disorders: microRNA gets motoring. NAT REV NEUROSCI 15(2), 67.

Li, X., Li, D., Zhou, W., Chai, Y., Yuan, R., Xiang, Y., 2015. A microRNA-activated molecular machine for non-enzymatic target recycling amplification detection of microRNA from cancer cells. Chem Commun (Camb) 51(55), 11084-11087.

Lin, S., Gregory, R.I., 2015. MicroRNA biogenesis pathways in cancer. NAT REV CANCER 15(6), 321-333.

Liu, L., Song, C., Zhang, Z., Yang, J., Zhou, L., Zhang, X., Xie, G., 2015. Ultrasensitive electrochemical detection of microRNA-21 combining layered nanostructure of oxidized single-walled carbon nanotubes and nanodiamonds by hybridization chain reaction. BIOSENS BIOELECTRON 70, 351-357.

Luo, M., Li, N., Liu, Y., Chen, C., Xiang, X., Ji, X., He, Z., 2014. Highly sensitive and multiple DNA biosensor based on isothermal strand-displacement polymerase reaction and functionalized

magnetic microparticles. BIOSENS BIOELECTRON 55, 318-323.

Manriquez, R., Lopez-Dellamary, F.A., Frydel, J., Emmler, T., Breitzke, H., Buntkowsky, G., Limbach, H.H., Shenderovich, I.G., 2009. Solid-state NMR studies of aminocarboxylic salt bridges in L-lysine modified cellulose. J PHYS CHEM B 113(4), 934-940.

Pers, Y.M., Jorgensen, C., 2013. MicroRNA in 2012: Biotherapeutic potential of microRNAs in rheumatic diseases. NAT REV RHEUMATOL 9(2), 76-78.

Preechaworapun, A., Dai, Z., Xiang, Y., Chailapakul, O., Wang, J., 2008. Investigation of the enzyme hydrolysis products of the substrates of alkaline phosphatase in electrochemical immunosensing. TALANTA 76(2), 424-431.

Radi, A.E., Acero, S.J., Baldrich, E., O'Sullivan, C.K., 2005. Reusable impedimetric aptasensor. ANAL CHEM 77(19), 6320-6323.

Radwan, S.H., Azzazy, H.M., 2009. Gold nanoparticles for molecular diagnostics. EXPERT REV MOL DIAGN 9(5), 511-524.

Shi, C., Liu, Q., Ma, C., Zhong, W., 2014. Exponential strand-displacement amplification for detection of microRNAs. ANAL CHEM 86(1), 336-339.

Shi, K., Dou, B., Yang, C., Chai, Y., Yuan, R., Xiang, Y., 2015. DNA-Fueled Molecular Machine Enables Enzyme-Free Target Recycling Amplification for Electronic Detection of MicroRNA from Cancer Cells with Highly Minimized Background Noise. ANAL CHEM 87(16), 8578-8583.

Situ, B., Cao, N., Li, B., Liu, Q., Lin, L., Dai, Z., Zou, X., Cai, Z., Wang, Q., Yan, X., Zheng, L., 2013. Sensitive electrochemical analysis of BRAF V600E mutation based on an amplification-refractory mutation system coupled with multienzyme functionalized Fe3O4/Au nanoparticles. BIOSENS BIOELECTRON 43, 257-263.

Valoczi, A., Hornyik, C., Varga, N., Burgyan, J., Kauppinen, S., Havelda, Z., 2004. Sensitive and specific detection of microRNAs by northern blot analysis using LNA-modified oligonucleotide probes. NUCLEIC ACIDS RES 32(22), e175.

Wang, C., Hu, J., Lu, M., Gu, H., Zhou, X., Chen, X., Zen, K., Zhang, C.Y., Zhang, T., Ge, J., Wang, J., Zhang, C., 2015. A panel of five serum miRNAs as a potential diagnostic tool for early-stage renal cell carcinoma. Sci Rep 5, 7610.

Wang, J.X., Zhang, X.J., Li, Q., Wang, K., Wang, Y., Jiao, J.Q., Feng, C., Teng, S., Zhou, L.Y., Gong, Y., Zhou, Z.X., Liu, J., Wang, J.L., Li, P.F., 2015. MicroRNA-103/107 Regulate Programmed Necrosis and Myocardial Ischemia/Reperfusion Injury Through Targeting FADD. CIRC RES 117(4), 352-363.

Wang, X., Hou, T., Lu, T., Li, F., 2014. Autonomous exonuclease III-assisted isothermal cycling signal amplification: a facile and highly sensitive fluorescence DNA glycosylase activity assay. ANAL CHEM 86(19), 9626-9631.

Wilson, M.S., Rauh, R.D., 2004. Hydroquinone diphosphate: an alkaline phosphatase substrate that does not produce electrode fouling in electrochemical immunoassays. BIOSENS BIOELECTRON 20(2), 276-283.

Yao, B., Liu, Y., Tabata, M., Zhu, H., Miyahara, Y., 2014. Sensitive detection of microRNA by chronocoulometry and rolling circle amplification on a gold electrode. Chem Commun (Camb) 50(68), 9704-9706.

Zhang, P., Wu, X., Chai, Y., Yuan, R., 2014. An electrochemiluminescent microRNA biosensor based on hybridization chain reaction coupled with hemin as the signal enhancer. ANALYST 139(11), 2748-2753.

Zhu, X., Shen, Y., Cao, J., Yin, L., Ban, F., Shu, Y., Li, G., 2015. Detection of microRNA SNPs with ultrahigh specificity by using reduced graphene oxide-assisted rolling circle amplification. Chem Commun (Camb) 51(49), 10002-10005.

Zou, B., Song, Q., Wang, J., Liu, Y., Zhou, G., 2014. Invasive reaction assisted strand-displacement signal amplification for sensitive DNA detection. Chem Commun (Camb) 50(89), 13722-13724.

Captions and legends

Table 1. Optimization of the different experimental variables affecting the determination of miR-21.

Fig.1. Representative diagram for the isothermal amplification-electrochemical sensing assay of miRNA. (A) ISDPR amplification with biotin label. (B) The fabrication process of the multienzyme functionalized MMCs and oxidation of ascorbic acid at an SPCE.

Fig.2. The fluorescence intensities of (A) various target miRNA concentrations, from 1 nM to 1 μM in the presence of phi29 polymerase, and (B) the same concentration of target miRNA in the presence and in the absence of phi29 polymerase.

Fig.3. Characterization by confocal microscopy: (A) fluorescence image of MMCs, (B) micrograph of MMCs, (C) fluorescence image of MMCs modified by FAM-probes, (D) micrograph of MMCs modified by FAM-probes. (E) Cyclic voltammograms in 10 mM K3[Fe(CN)6]:K4[Fe(CN)6] (1:1) mixture containing 0.1 M KCl at bare SPCE (a) MMC, (b) MMC/probe, (c) MMC/bio-DNA, (d)

MMC/bio-DNA/Sa-ALP.

Fig.4. (A) DPV responses for different target miRNA-21 concentrations: (a) 10^{-8} M, (b) 10^{-9} M, (c) 10^{-10} M, (d) 10^{-11} M, (e) 10^{-12} M, (f) 10^{-13} M, (g) 10^{-14} M, (h) blank, (B) The relationship between current and the logarithm of target oligonucleotide sequence, plotted with the data of Fig. 4A, (C) Selectivity of the proposed method where the concentration of each is 10 nM: (a) random RNA, (b) TM miR-21, (c) SM miR-21, (d) miR-21.

Fig.5. Analysis of miR-21 in human breast tissues and paired adjacent tissues. The bars represent the content of miR-21 in total RNA from five pairs of cancer tissue and paired adjacent tissue of five people diagnosed with breast cancer measured by the sensor method and by PCR, respectively.

Highlights

A novel electrochemical sensing method for miRNA detection was established.
A dual amplification strategy of ISDPR and multienzyme functionalized nanoparticles was developed and evaluated.
This method doesn't need reverse transcription and large equipment and have a shorter time to suit widely application in primary hospital.

Table 1.Optimization of the different experimental variables affecting the

determination of miR-21.

Variable	Range tested	Selected value
MMP	1-15μl	5μl
Phi29 polymerase	0.5-3.5μl	2μl
Incubation time of ISDPR	40-160min	120min
Incubation time of	5-35min	15min
Strep-ALP		

Figure 1

Figure 2

Figure 3

Figure 4

Figure5